Bistable self-organization of nuclear spins in conducting solids

Didier Gerbault and Didier Gourier*
Ecole Nationale Supérieure de Chimie de Paris, Laboratoire de Chimie Appliquée de l'Etat Solide, 11 rue Pierre et Marie Curie, 75231 Paris CEDEX 05, France
(Received 27 March 1996)

Under suitable conditions the dynamic nuclear polarization by the Overhauser effect in conductors is responsible for a bistable hysteresis of the electron spin resonance (ESR) line of conduction electrons [Phys. Rev. B **47**, 15 023 (1993)]. We study in this work the dynamics of the phenomenon in terms of the bistable self-organization of nuclear spins and the microwave field. The deterministic evolution of the nuclear field is described as an overdamped motion in a potential U. It is shown that the shape of the ESR line, in both monostable and bistable regimes, is proportional to the second derivative of this potential. By taking into account the fluctuations of the nuclear field, a Schrödinger equation for the self-organized spin-field system is derived. For the monostable Overhauser effect, this equation is that of the quantum mechanical harmonic oscillator. The self-organized spin-field system can thus be compared with a ''vibrating molecule'' in the nuclear field space, in which the steady state nuclear field corresponds to the equilibrium ''interatomic distance.'' With this analogy, the bistable spin-field system may also be compared to a ''mixed valence molecular complex,'' in which the two stable configurations of the ''complex'' correspond to the two stable steady states of the nuclear field. [S0163-1829(96)04433-5]

I. INTRODUCTION

An ensemble of noninteracting free electrons in the conduction band of a metal or a semiconductor submitted to a static magnetic field B_0 provides a very simple case of a two-level quantum system. The transition between the two electron spin states upon interaction with an electromagnetic field B_1 of frequency ν in the microwave range, called conduction electron spin resonance (CESR), is characterized by a single resonance line with a symmetrical Lorentzian shape.[1] When the solid contains chemical elements with nonzero nuclear spins I, the polarization $\langle I_z \rangle$ of the nuclei in the static field is nonzero according to the Boltzmann law, so that the effective magnetic field seen by the electron spins is the sum of the external field B_0 and the nuclear field B_n resulting from the nuclear polarization. Thus the thermal nuclear polarization induces a shift of the electron spin states. The thermal equilibrium value of B_n is generally very small, at least at high temperatures. However it can be considerably enhanced by saturation of the CESR. This effect has been predicted in metals by Overhauser[2] and analyzed theoretically by Solomon.[3] It has also been experimentally observed in metals,[4] semiconductors,[5] and organic conductors.[6] The Overhauser effect manifests itself by a shift and a distortion of the CESR line which can be directly observed by ESR if B_n is sufficiently high, and requires electron nuclear double resonance (ENDOR) spectroscopy if B_n is of the order of a few mG, such as in organic conductors.[6]

This Overhauser effect is monostable, which means that it exhibits only one stable state for the nuclear field B_n. The consequence is that the CESR exhibits no hysteresis and the signals recorded by increasing or decreasing B_0 are identical. This is the general situation encountered so far (discontinuous line in Fig. 1.) However, under certain circumstances, the Overhauser effect becomes bistable, which means that two stable states of the nuclear field may coexist for the same values of the external parameters (or control parameters) B_0, B_1, and the temperature T. This effect has been suggested by Kaplan[7] and qualitatively observed by Gueron and Ryter in metallic lithium particles at 4 K.[8] A strong bistability has been recently observed at high temperature and analyzed in detail by Aubay and Gourier in β-Ga_2O_3.[9,10] The latter compound is an n-type semiconductor when slightly oxygen deficient, the oxygen vacancies acting as shallow donors. Bistability originates from a feedback loop connecting the saturation of the CESR line and the nuclear field created by saturation. It occurs when the dynamical shift of the CESR line is larger than the natural width of this line. This highly nonlinear effect is responsible for a bending of the CESR line, which takes a ''shark fin'' shape (full line in Fig. 1). It can be seen that there is a finite field range $B_0^{\downarrow} < B_0 < B_0^{\uparrow}$

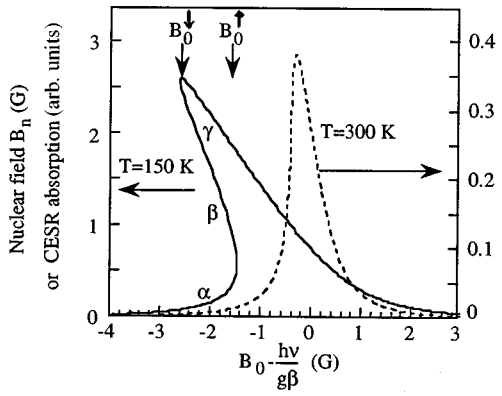

FIG. 1. Calculated nuclear field and CESR absorption for β-Ga_2O_3 at 150 K (full line) and 300 K (discontinuous line) vs the external magnetic field. The material parameters are $T_1 \approx T_2 \approx 2\times10^{-7}$ s, $T_x \approx 0.5$ s, $(\Delta B_{0\nu})_{max}=5$ G (at 150 K) and $(\Delta B_{0\nu})_{max}=2$ G (at 300 K). The control parameters are $B_1=0.4$ G (at 150 K) and $B_1=0.14$ G (at 300 K).

where the CESR intensity takes three values I_α, I_β, and I_γ. Only I_α and I_γ can be observed experimentally by sweeping up and down the magnetic field. The branch α is recorded upon a positive variation of B_0, and undergoes a transition to the γ state at the critical field $B_0^{\uparrow}$. Upon negative variation of B_0, the system occupies first the γ state and undergoes a transition $\gamma \rightarrow \alpha$ at a critical field $B_0^{\downarrow} < B_0^{\uparrow}$. Thus the bistable Overhauser effect manifests itself by a hysteresis of the CESR line, which will be hereafter referred to as bistable conduction electron spin resonance (BCESR). This effect is easily produced in β-Ga_2O_3 under moderate external field ($B_0 \approx 3400$ G) and moderate saturation conditions at temperature as high as room temperature.[10] The reason is that this solid possesses optimal electronic and chemical structures which ensure a narrow CESR line, together with an efficient dynamical shift of the resonance.[11] CESR of gallium oxide thus offers an ideal tool for a detailed investigation of the bistable Overhauser effect. It should be noticed that this effect is a general property of electronic conductors containing nuclear spins. However most solids which exhibit or are liable to exhibit this effect require very low temperatures and sometimes a high external field B_0.[12]

From the point of view of synergetics,[13] the Overhauser effect may be described as the self-organization of a system composed of nuclear spins, electron spins, and the microwave field B_1. However in a semiconductor such as gallium oxide, the concentration of unpaired electron spins[10] ($\approx 10^{18}$ cm^{-3}) is much smaller than the concentration of nuclear spins ($\approx 10^{22}$ cm^{-3}), so that unpaired electrons may be considered as impurities. Restricting the phenomenon to its major components, it may be considered as a self-organization of the nuclear spins and the field B_1. This highly organized spin-field system shows instabilities with a first-order transition having its usual bistability and hysteresis.

The aim of the present work is to propose a description of the bistable Overhauser effect by focusing on the deterministic as well as the stochastic aspects of the dynamics of the nuclear field. Recently Gourier *et al.*[14] showed that the differential equation governing the dynamics of the nuclear polarization is similar to that of an overdamped motion in a potential. In this work we introduce the fluctuation effects of the nuclear field which are unavoidable because of the relatively small size of the electron-spin–nuclear-spin system, and derive a Hamiltonian for the self-organized spin-field system which bears many similarities with the vibrational Hamiltonian of simple molecular systems. In particular we show that the monostable Overhauser effect is described by the same quantum-mechanical harmonic oscillator as that of a vibrating diatomic molecule, where the nuclear field B_n substitutes the configuration coordinate (the interatomic distance). Within this framework, the bistable Overhauser effect is equivalent to a mixed-valence molecular architecture, which has been recently proposed by Guihery *et al.* for bit storage applications.[15]

Due to the optimal conditions offered by β-Ga_3O_3 for the study of both monostable and bistable Overhauser effects by ESR spectroscopy at high temperatures, we used this compound as a model in this work. This paper is arranged as follows. A brief description of the experimental conditions is first given in Sec. II, and the basic principles of monostable and bistable Overhauser effect are recalled in Sec. III. After the definition in Sec. IV of the characteristic times controlling the dynamics of the phenomenon, the deterministic aspect of the dynamics is described in Sec. V with the introduction of the dynamic potential characterizing the Overhauser effect. In particular it is shown that the CESR intensity (the first derivative of the absorption line) is directly related to the second derivative of this potential. The effect of fluctuations of the nuclear polarization is introduced in Sec. VI, by setting the Fokker-Planck equation (FPE) of the fluctuating nuclear field. Its resolution gives the stationary distribution of B_n. In Sec. VII the FPE of the self-organized spin-field system is transformed into a Schrödinger equation which is analyzed for both monostable and bistable situations. Finally, the analogy of the monostable and bistable self-organized spin-field systems with diatomic and mixed-valence molecular architectures is developed in Sec. VIII.

II. EXPERIMENTAL SECTION

All the CESR spectra were recorded on single crystals of oxygen-deficient β-Ga_2O_3. The crystal was grown and the sample prepared according to the usual procedure.[10] Very thin platelets (thickness <0.1 mm) were used in order to avoid skin depth distortion of the CESR line.[1] The concentration of unpaired conduction electron spins $N_s \approx 10^{18}$ cm^{-3} was determined by comparison with a standard diphenylpicrylhydrazyl (DPPH) sample.[10] The CESR spectra were recorded at the X band on a Bruker 220 D spectrometer equipped with a variable temperature device. The crystals were oriented in the ESR cavity with the crystallographic axis **b** parallel to B_0. With this orientation, the unsaturated CESR line is characterized by $g = 1.963(5)$, and a linewidth $\Delta B = 0.4$ G in the range 300–150 K which increases below 150 K. Most of the CESR spectra were recorded at 150 K with a microwave field amplitude $B_1 \approx 0.4$ G, which corresponds to the optimal conditions for observing BCESR.[10] The pertinent parameters of gallium oxide at this temperature are the electronic relaxation times $T_1 \approx T_2 \approx 2 \times 10^{-7}$ s, and $(\Delta B_{0\nu})_{\max} \approx 5$ G. The latter parameter represents the highest nuclear field attainable at this temperature. Monostable CESR spectra were recorded at room temperature [$T_1 \approx T_2 \approx 2 \times 10^{-7}$ s, and $(\Delta B_{0\nu})_{\max} \approx 2$ G] at a microwave field value $B_1 \approx 0.14$ G, just below the bistability threshold.[10]

Magnetic switch experiments, where B_0 can be rapidly changed in less than a microsecond, were performed according to the procedure described in Ref. 14.

III. PRINCIPLES OF MONOSTABLE AND BISTABLE OVERHAUSER EFFECT

A conduction-electron spin S delocalized in the conduction band of a conducting solid, submitted to a static magnetic field B_0 and a microwave field B_1 of frequency ν, is characterized by the resonance condition $h\nu = g\beta B_0$, where g and β are, respectively, the electron g factor and the electron Bohr magneton. If the solid contains a chemical element with nonzero nuclear spin I, the thermal equilibrium nuclear polarization creates a nuclear field B_n which adds itself to the external field B_0. The resonance condition becomes

$$h\nu = g\beta(B_0 + B_n). \tag{1}$$

The thermal equilibrium value of B_n is very small near room temperature (for example, $B_n \approx 4\times10^{-3}$ G at 150 K for β-Ga_2O_3 in a field $B_0 \approx 3400$ G), so that it can be neglected in expression (1). However the nuclear field can be considerably enhanced by dynamic nuclear polarization (Overhauser effect) induced by saturation of the resonance line.[2] This enhanced nuclear field modifies the resonance condition (1) since the latter is now fulfilled at a lower value of B_0. The saturation and the nuclear field are connected by a feedback loop since the dynamical shift of the resonance modifies the saturation condition, which modifies in turn the resulting nuclear field, and so on. A nonlinear effect of the magnetic resonance—the saturation of the CESR line—is thus combined with the feedback produced by the dynamic polarization of nuclear spins, which makes the nuclear field a function of itself, $B_n = f(B_n)$.[9] The detailed expression of this self-consistent equation is derived by the combination of the Bloch equation for the resonance[16] and from the Overhauser equation for the nuclear field:[2]

$$B_n = (\Delta B_{0\nu})_{\max} \frac{\gamma^2 T_1 T_2 B_1^2}{1+\gamma^2 T_2^2 (B_n + B_0 - h\nu/g\beta)^2 + \gamma^2 T_1 T_2 B_1^2}. \tag{2}$$

T_2 and T_1 are, respectively, the spin-spin and the spin-lattice relaxation times of conduction electrons. The parameter $(\Delta B_{0\nu})_{\max}$ corresponds to the largest accessible value of B_n, which is achieved for complete saturation ($\gamma^2 T_1 T_2 B_1^2 \gg 1$) and at the resonance condition given by expression (1). $(\Delta B_{0\nu})_{\max}$ is given by the following expression:[17]

$$(\Delta B_{0\nu})_{\max} = \frac{I(I+1)NAB_0}{3kT} f, \tag{3}$$

where N is the number of nuclear spins I interacting with each electron and A is the hyperfine interaction for each nucleus. The leakage factor f (with $0 \leqslant f \leqslant 1$) reflects the efficiency of the dynamic nuclear polarization mechanism.[3]

Expression (2) is a third degree equation which exhibits either one, two, or three solutions for B_n, depending on parameters $(\Delta B_{0\nu})_{\max}$, T_1 and T_2 which are determined by the chemical and the electronic structures of the compound (T_1, T_2, I, and NAf) and by the control parameter (B_0, B_1, and T). When T_2 and $(\Delta B_{0\nu})_{\max}$ are too small to allow three solutions for Eq. (2), the Overhauser effect is monostable, and the CESR absorption is a more or less distorted Lorentzian line shifted to low magnetic field by the nuclear field B_n (Overhauser shift). An example is shown in Fig. 2 (discontinuous line) for β-Ga_2O_3 at room temperature. For this compound between 4 K and room temperature, and for several electronic conductors at liquid-helium temperature,[12] T_2 and $(\Delta B_{0\nu})_{\max}$ are sufficiently large to allow three solutions for B_n. In that case the curve $B_n = f(B_0)$ takes a ''shark fin'' shape, as shown in Fig. 1 for β-Ga_2O_3 at 150 K. It should be noticed that the microwave power absorbed by the sample is proportional to the nuclear field,[10] so that Fig. 1 also represents the BCESR absorption line shape. The ESR signal being detected by modulation of the magnetic field B_0, the ESR intensity $I_{\rm ESR}$ takes the form of the first derivative of the absorption line. For electron spins submitted to the Overhauser effect, the CESR intensity (monostable and bistable) is given by the following expression:[10]

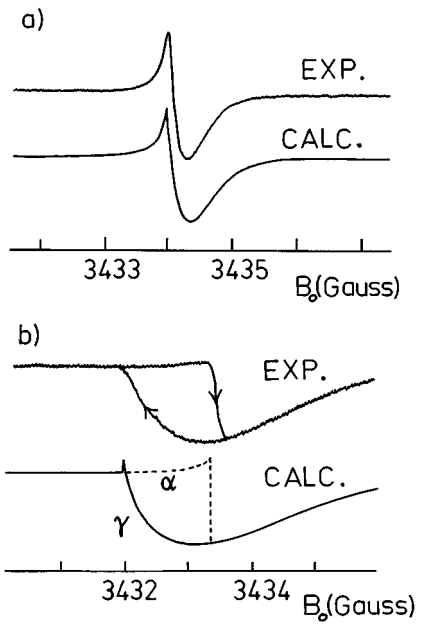

FIG. 2. Experimental and calculated CESR spectra for β-Ga_2O_3 at 300 K (a) and 150 K (b). Sweeping time: 100 s. The parameters are the same as in Fig. 1.

$$I_{\rm ESR} = -I_0 \frac{B_1(B_0 + B_n - h\nu/g\beta)}{[1+\gamma^2 T_2^2 (B_0 + B_n - h\nu/g\beta)^2 + \gamma^2 T_1 T_2 B_1^2]^2}, \tag{4}$$

B_n being a solution of Eq. (2). The constant I_0 depends on both the spectrometer and the sample. Expression (4) allows very accurate simulations of bistable and monostable CESR lines.[10] Figure 2 shows an example of experimental and calculated BCESR lines recorded at the X band in both monostable and bistable regimes for a single crystal of β-Ga_2O_3. It is important to note that bistability distorts the CESR line in such a way that the first derivative of the absorption corresponding to the α-state (forward sweep of B_0) and to the γ state (backward sweep of B_0) occurs only on one side of the baseline. The unstable β state occupies the other side, but it cannot be observed under magnetic field sweeping conditions.

IV. TIME SCALE OF BCESR

Since the primary objective of this paper is the investigation of the dynamics of the bistable Overhauser effect, it is first necessary to identify the different characteristic times which influence or control the phenomenon (Fig. 3).

The first time constant to be considered is the correlation time τ_c of the mobile electron at the nuclear site of the conductor. It is generally of the order of $\tau_c \approx 10^{-14}$ s $\ll h/A$, where A is the Fermi contact hyperfine interaction of the electron spin with the nucleus. This inequality is at the origin of the motional averaging of the CESR spectrum, which is reduced to a single Lorentzian line.

The second set of time constants contains the electron spin-lattice relaxation time T_1 and the electron spin-spin re-

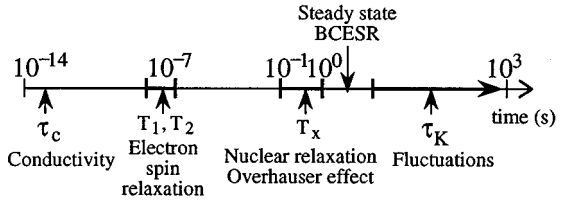

FIG. 3. Characteristic times of BCESR.

laxation time T_2. The extreme narrowing regime of the CESR line is characterized by the equality $T_1 \approx T_2$. However these two relaxation times do not play the same role in the establishment of the nuclear order. A long T_1 is needed for an easy saturation of the resonance line, which in turn produces the enhancement of the nuclear field B_n by the dynamic nuclear polarization.[2] The relaxation time T_2 essentially controls the number of solutions of Eq. (2). A bistable situation needs a long T_2, which corresponds to a narrow CESR line. Gallium oxide above 150 K is characterized by $T_1 \approx T_2 \approx 2 \times 10^{-7}$ s, which ensures conditions for obtaining three stationary solutions for the nuclear field in Eq. (2).

The time constant for the establishment of the nuclear polarization is the nuclear relaxation time T_x corresponding to simultaneous flips of electron and nuclear spins in opposite directions, characterized by the selection rule $\Delta(m_s + m_I) = 0$. This relaxation is responsible for the transfer of the electron spin polarization to nuclear spins, giving a nonequilibrium nuclear polarization. T_x must be shorter than the other nuclear spin-lattice relaxation times T_{1n} in order to produce an efficient nonequilibrium nuclear polarization. In β-Ga_2O_3 above 150 K, T_x is of the order of 0.1 to 0.5 s while T_{1n} is of the order of 1 to 10 s.[18] The higher the difference between T_x and T_{1n}, the best the efficiency of the dynamic nuclear polarization, determined by the leakage factor f given by the following expression:[3]

$$f = \frac{1/T_x}{1/T_x + 1/T_{1n}} \tag{5}$$

with $0 \leqslant f \leqslant 1$. For a given electronic conductor, f determines the amplitude of the nuclear field $(\Delta B_{0\nu})_{\max}$ [see expression (3)] which also controls the number of solutions of Eq. (2) and thus the existence of bistability.

Bistable systems are sensitive to fluctuations, which are able to induce transitions between the two stable stationary states. These fluctuations thus determine the long-time behavior of BCESR as it will be seen in Sec. V. The characteristic time of fluctuations, called the Kramers time τ_K,[19] depends on the values of the different control parameters T, B_0, and B_1. It must be larger than the nuclear relaxation time T_x for the observation of bistability by a sweep of a control parameter.

Consequently, obtaining a BCESR such as that presented in Fig. 3 requires two conditions: (i) the spin system should stay in a steady-state nuclear field, characterized by $\partial B_n/\partial t = 0$, during the magnetic field sweep through the resonance; (ii) the fluctuations should be sufficiently weak to avoid $\alpha \leftrightarrow \gamma$ switching during the sweep. These two conditions are fulfilled if the sweeping rate through the resonance is sufficiently slow to ensure a steady-state nuclear field, and sufficiently rapid to avoid the effect of fluctuations. As will be shown below, this condition is easily verified in β-Ga_2O_3 because $\tau_K \gg T_x$ in this compound (Fig. 4). Therefore a description of BCESR spectra recorded with very slow or very fast field sweep conditions needs to include the dynamics of the nuclear field. This topic is dealt with in the later parts of this paper.

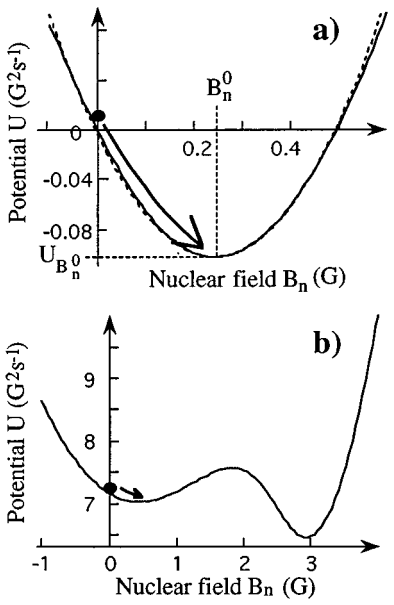

FIG. 4. Examples of potentials U for β-Ga_2O_3. (a) $T = 300$ K, $B_1 = 0.14$ G, and $B_0 \approx h\nu/g\beta$. The discontinuous line represents the harmonic approximation for the potential. (b) $T = 150$ K, $B_1 = 0.4$ G, $B_0 - h\nu/g\beta = -2.6$ G. The other parameters are $T_1 \approx T_2 \approx 2 \times 10^{-7}$ s, $T_x \approx 0.5$ s, and $(\Delta B_{0\nu})_{\max} = 2$ G.

V. DETERMINISTIC DYNAMICS OF THE NUCLEAR FIELD

A. Description by a potential

Let us first consider the situation corresponding to a passage time through the resonance which is smaller than the nuclear relaxation time T_x. This situation also includes the effect of rapid switching of one of the control parameters B_0, B_1, or T. Since the steady-state condition $\partial B_n/\partial t = 0$ is not valid in this case, the evolution of B_n must be taken into account in the description of the bistable resonance.

The rate equation for the nuclear polarization $\langle I_z \rangle = g\beta B_n/NA$ is given by the formula[20]

$$\frac{\partial \langle I_z \rangle}{\partial t} = -\frac{1}{T_x}\left(\langle I_z \rangle - \langle I_z^0 \rangle - \langle I_z^0 \rangle \frac{g\beta}{g_n \beta_n} fs \right)$$

with[10]

$$s = \frac{\gamma^2 T_1 T_2 B_1^2}{1 + \gamma^2 T_1 T_2 B_1^2 + \gamma^2 T_2^2 (B_0 + B_n - h\nu/g\beta)^2}, \tag{6}$$

where $\langle I_z^0 \rangle = g_n \beta_n I(I+1) B_0/3kT$ is the thermal equilibrium nuclear polarization. Under saturation conditions ($s > 0$), Eq. (6) with $g\beta fs/g_n\beta_n \gg 1$ gives the following one-dimensional differential equation which governs the deterministic evolution of B_n:

$$T_x \frac{\partial B_n}{\partial T} + B_n = (\Delta B_{0\nu})_{\max} \times \frac{\gamma^2 T_1 T_2 B_1^2}{1+\gamma^2 T_1 T_2 B_1^2 + \gamma^2 T_2^2 (B_0 + B_n - h\nu/g\beta)^2}. \tag{7}$$

Equation (7) with the steady-state condition $\partial B_n/\partial t = 0$ gives the fundamental equation (2) of the nuclear field. The two important characteristics of Eq. (7) are that it is a continuous function of control parameters B_0 and B_1, and that it is autonomous if we neglect the time dependence of B_0 resulting from the modulation in the detection of the ESR signal. The latter assumption is reasonable since the modulation frequency (100-kHz) is much larger than the relaxation frequency (2–10 Hz), which implies that the nuclear field cannot follow the magnetic field modulation.[10] The consequence of the particular form of Eq. (7) is that the evolution of the nuclear polarization may be interpreted as the *overdamped motion of a fictitious particle*[21] in a potential U defined by

$$\frac{\partial B_n}{\partial t} = -\frac{\partial U}{\partial B_n}, \tag{8}$$

where $-\partial U/\partial B_n$ is the damping force. The number of steady states for B_n, which satisfy the condition $\partial B_n/\partial t = 0$, is determined by the number of extrema of the potential U, corresponding to $\partial U/\partial B_n = 0$. Integration of Eq. (7) gives the following general expression for the dynamic potential U:.

$$U(B_n) = -\int \frac{\partial B_n}{\partial t}\, dB_n = \frac{B_n^2}{2T_x} - \frac{(\Delta B_{0\nu})_{\max} \gamma T_1 B_1^2}{T_x (1+\gamma^2 T_1 T_2 B_1^2)^{1/2}} \times \arctan\left[\frac{\gamma T_2 (B_0 + B_n - h\nu/g\beta)}{(1+\gamma^2 T_1 T_2 B_1^2)^{1/2}}\right]. \tag{9}$$

This potential always has one minimum if $(\Delta B_{0\nu})_{\max} < 4/\gamma T_2$ and may have two minima if $(\Delta B_{0\nu})_{\max} < 4/\gamma T_2$. The mechanical analogy of this self-organized spin-field system may become obvious if we consider the usual situation of a monostable Overhauser effect, exemplified by the unsaturated resonance line ($\gamma^2 T_1 T_2 B_1^2 \ll 1$) of β-Ga_2O_3 at 300 K and for an external field B_0 close to the resonance condition $B_0 + B_n \approx h\nu/g\beta$. The potential U is represented by the full line in Fig. 4(a). It can be expressed by the following expansion of Eq. (9) about the steady-state value B_n^0 of the nuclear field solution of Eq. (2). By limiting the expansion to the second order in B_n, we obtain

$$U(B_n) \approx U(B_n^0) + \frac{1}{2} U''_{B_n^0} (B_n - B_n^0)^2. \tag{10}$$

This harmonic expression of $U(B_n)$ is represented by the dotted line in Fig. 4(a). The self-organized spin-field system can be considered to behave as a one-dimensional motion of a particle submitted to the damping force $F = U''_{B_n^0}(B_n^0 - B_n)$. Let us now consider that the system is at thermal equilibrium ($B_1 = 0$) at $t < 0$, so that the initial nuclear field is $B_n(t<0) \approx 0$. At $t = 0$, the microwave field is rapidly switched (within a time $\delta t \ll T_x$) to its final value B_1, which generates the potential $U(B_n)$ with the ''spin-field particle'' still characterized by its initial value $B_n(t=0) \approx 0$. The nuclear field will then evolve towards its steady state B_n^0, as represented by the arrow in Fig. 4(a).

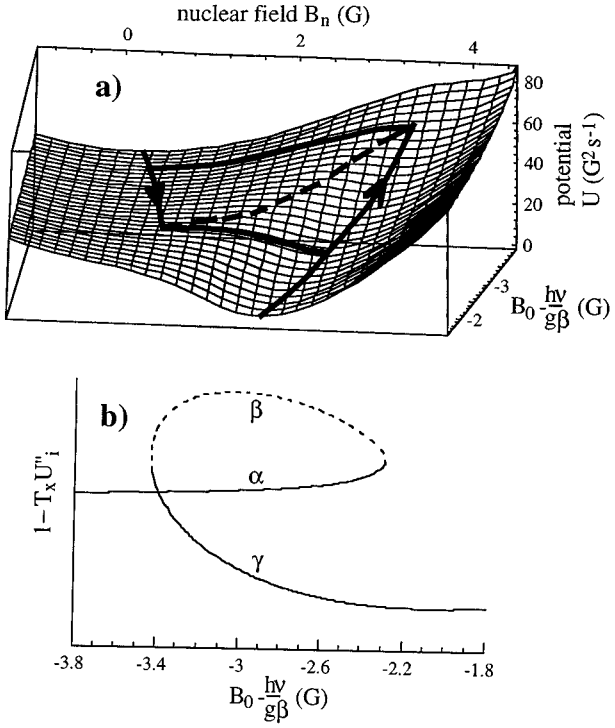

FIG. 5. (a) Three-dimensional plot of the dynamic potential U for β-Ga_2O_3 at 150 K vs the external field B_0. The parameters of the calculation are the same as for Fig. 4(b). The thick lines corresponding to the minima of the potential represent the trajectory of the spin-field system during upward and downward magnetic field sweeps. The discontinuous line represents the position of the potential maxima. (b) Variation of $1 - T_x U''_i$ vs the external field B_0, where U''_i ($i = \alpha, \beta, \gamma$) represents the second derivative of the potential at its minima (full line) and at its maximum (discontinuous line).

In a more general situation, where the restrictive conditions $\gamma^2 T_1 T_2 B_1^2 \ll 1$ and $B_0 + B_n \approx h\nu/g\beta$ are absent, the potential cannot be expanded in power series, and expression (9) should be used as such. In the case of bistability, characterized by $(\Delta B_{0\nu})_{\max} > 4/\gamma T_2$ and $B_0^{\downarrow} < B_0 < B_0^{\uparrow}$, the potential U has two minima corresponding to the stable steady-state nuclear fields B_n^{α} and B_n^{γ}, and one maximum at B_n^{β} corresponding to the third (unstable) steady state. An example of a bistable potential is shown in Fig. 4(b). As for the harmonic potential, if the microwave field B_1 is switched from zero to its final value at $t = 0$, generating the potential U, the fictitious particle is first at an initial potential $U(B_n = 0)$. It next moves towards the steady state α and remains trapped in this state if there is no fluctuation, despite the fact that the state γ is the most stable.

It is now easy to understand the behavior of the spin-field system during a magnetic field sweep corresponding to a BCESR spectrum, by considering Figs. 2(b) and 5(a). The latter represents a three-dimensional plot of the potential U as a function of B_n and B_0. The trajectory of the spin-field

system during a slow sweep of B_0 (ensuring the steady-state condition $\partial B_n/\partial t \approx 0$) follows adiabatically the potential valleys. It is represented by full lines in Fig. 5(a). In the field range $B_0^{\downarrow} < B_0 < B_0^{\uparrow}$ corresponding to the bistable conditions, the trajectory depends on the sweep direction (the sign of dB_0/dt). Upon increasing the variation of B_0, the spin-field system remains in the α state as long as the potential barrier exists. At the critical field $B_0^{\uparrow}$ where the potential barrier vanishes (corresponding to $U_\alpha = U_\beta > U_\gamma$), the spin-field system follows the transition $\alpha \rightarrow \gamma$. Upon decreasing field variation, the transition $\gamma \rightarrow \alpha$ occurs at a lower critical field $B_0^{\downarrow}$, corresponding to $U_\gamma = U_\beta > U_\alpha$. However the transitions $\alpha \rightarrow \gamma$ and $\gamma \rightarrow \alpha$ are not so abrupt, as can be seen by comparing the experimental and calculated BCESR spectra shown in Fig. 2. This is because fluctuations of B_n can induce the switching even if the potential barrier has not completely vanished. The effect of fluctuations will be considered in Sec. VI.

B. General expression of the CESR intensity

It was pointed out above that in the bistable regime, the BCESR spectrum (α and γ states) appears only on one side of the baseline, while the (theoretical) spectrum of the β state lies on the other side as shown in Fig. 2. This dissymmetry is surprising, the CESR spectrum being the first derivative of the microwave power absorbed by the spin system. Its double integral, which gives the surface of the CESR line in a situation of monostability, becomes infinite in a situation of bistability. This unusual CESR line shape can be explained by comparing expressions (4) and (9), which give, respectively, the CESR intensity and the dynamic potential U of the self-organized spin-field system. These two expressions are related by

$$\frac{I_{\mathrm{ESR}}}{I_0} = 1 - T_x U''(B_n). \tag{11}$$

The consequence is that a simple examination of the shape of U gives a qualitative prediction of the steady state as well as the transient CESR intensities.

(i) During a magnetic field sweep under steady-state conditions, the CESR intensity is given by expression (11) where the second derivative of $U(B_n)$ is taken at the stationary states B_n^{α}, B_n^{β}, and B_n^{γ}. Figure 5(b) represents the dependence on the magnetic field of $1 - T_x U_i''$ $(i = \alpha, \beta, \gamma)$ corresponding to the potentials U of Fig. 5(a). These curves reproduce fairly well the shape of BCESR spectra as can be checked by comparison with Fig. 2(b). Since the signs of U_i'' at the minima and the maximum of the potential are different, the sign of the CESR intensity of the stable states α and γ is opposite to that of the unstable state β. Moreover the bistable potentials are always characterized by $|U_\gamma''| > |U_\alpha''| \approx 1/T_x$, so that the CESR intensity of the γ state (forward field sweep) is always larger than that of the α state (backward field sweep), which is close to zero. The peculiar shape of the BCESR spectra is thus completely determined by the curvature of the potential wells.

(ii) Expression (11) provides also a qualitative prediction of the CESR intensity in a transient experiment, for example

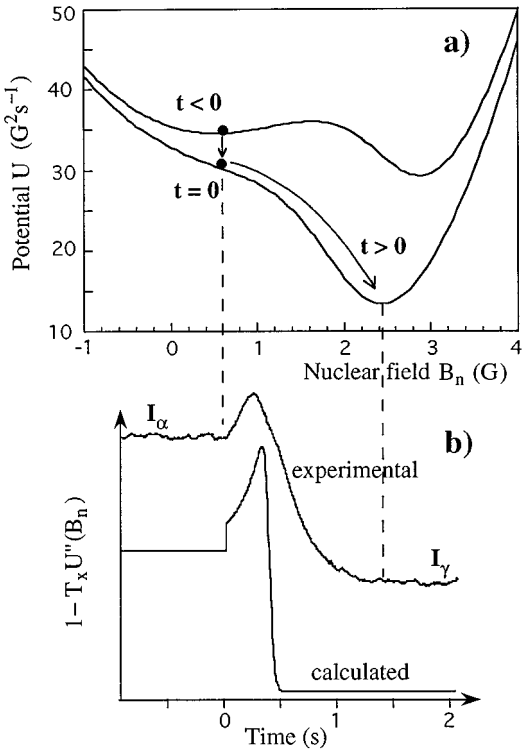

FIG. 6. Effect of a rapid variation of B_0 on the CESR intensity in β-Ga_2O_3 at 150 K with a microwave field $B_1 = 0.4$ G. The field is switched at $t = 0$. It takes the values $B_0 - h\nu/g\beta = -2.5$ G at $t < 0$ and $B_0 - h\nu/g\beta = -1.9$ G at $t \geqslant 0$. (b) Experimental and calculated time dependences of the CESR intensity. The spin system was prepared in the α state at $t < 0$. The other parameters of the calculation are those of β-Ga_2O_3 at 150 K.

when the spin-field system makes a transition from one stable state to another after a sudden variation of a control parameter. An example of the effect of an abrupt variation of B_0 is shown in Fig. 6. At $t < 0$, the spin-field system is prepared in the α state by a slow positive field sweep stopped at a value $B_0(t < 0)$ [upper potential in Fig. 6(a)]. This field is characterized by the nuclear field $B_n(t < 0) = B_n^{\alpha}$. At $t = 0$, the field B_0 is rapidly switched to a value $B_0(t = 0) \geqslant B_0^{\uparrow}$ corresponding to a situation of monostability, just above the transition $\alpha \rightarrow \gamma$. The corresponding potential is noted $U(t \geqslant 0)$ in Fig. 6(a). If the switching of B_0 occurs in a time scale smaller than T_x, the nuclear polarization cannot immediately follow the variation of B_0. This corresponds to the vertical transition between the two potentials represented in Fig. 6(a). After the field switching, the system evolves to the stationary state of the potential $U(t \geqslant 0)$ in a time scale of the order of the nuclear relaxation time. This potential has been chosen to differ significantly from a harmonic potential. In particular the sign of $U''(B_n)$ changes along the trajectory of the spin-field system toward its final state, as shown in Fig. 6(b). According to expression (11), this should correspond to a similar change of the CESR intensity during this evolution. The experimental time dependence of the CESR intensity shown in Fig. 6(b) is in qualitative agreement with this expectation.

VI. EFFECT OF FLUCTUATIONS

A. Fluctuations and long-time behavior of BCESR

At this stage of the investigation of the spin-field dynamics, it was assumed that the bistable nuclear field is strictly determined by the control parameters. However fluctuations cannot be avoided and will necessarily influence the dynamics by inducing $\alpha \leftrightarrow \gamma$ transition in the bistable potential. Local fluctuations of B_n can be induced by random flipping of nuclear spins. The manifestation of these fluctuations can be represented as follows. Let us consider a single electron spin S interacting with N nuclear spins I by a scalar interaction A. The nuclear field is given by $B_n = NA\langle I_z\rangle / g\beta$, where the nuclear polarization $\langle I_z\rangle$ is the ensemble average of the nuclear spins over the N nuclei. This nuclear polarization is maintained by the electron-nucleus relaxation mechanism corresponding to the relaxation time T_x. Since nuclear spins may also relax independently with a relaxation time $T_{In} > T_x$, the effect on the nuclear field of random flipping of one nuclear spin will depend on the total number N of nuclear spins, which represents the size of the spin system. If N is very large, this system may be considered as macroscopic, and independent flipping of nuclear spins do not strongly affect B_n. If N is small enough so that the spin system must be considered as microscopic, each independent nuclear spin flipping can modify significantly the nuclear polarization.

The important effect of fluctuations is to control the long-time behavior of BCESR by inducing transitions between α and γ states of the bistable potential in the presence of a potential barrier. In that case the final occupied state is always that possessing the lowest potential. In order to stress the effect of fluctuations of B_n in β-Ga_2O_3 under bistable conditions, let us consider the BCESR spectrum of Fig. 2. This spectrum was recorded with a sweeping rate large enough to prevent the effect of fluctuations, so that the spin system effectively occupies successively the two stationary states during the forward and backward field sweeps. However, if the external field is increased up to a value $B_0^{\downarrow} < B_0 < B_0^{\uparrow}$ inside the bistability window, and corresponding to the potential condition $U_\gamma < U_\alpha$, the system lies first in the α state, but fluctuations provoke the transition to the more stable γ state, which manifests itself by a variation of the CESR intensity. The result is shown in Fig. 7 for two values of B_0, where it can be seen that the fluctuation-induced $\alpha \rightarrow \gamma$ switching is achieved in a time scale which can be as high as 10^3 s. The kinetics of the transition is controlled by the intensity D of the fluctuations and by the internal parameters B_0, B_1 and T, which determine the height $U_\beta - U_{\alpha,\gamma}$ of the potential barrier. The effect of fluctuations has an important consequence on the BCESR itself. If the field is swept very slowly through the resonance line, the spin-field system always occupies the lowest potential during the field sweeping, so that the hysteresis vanishes.

Fluctuations of B_n can be accounted for in Eq. (8) by adding a random force $\eta(t)$ to the damping force $-\partial U/\partial B_n$, giving the following stochastic differential equation (Langevin equation):

$$\frac{\partial B_n}{\partial t} = -\frac{\partial U}{\partial B_n} + \eta(t). \tag{12}$$

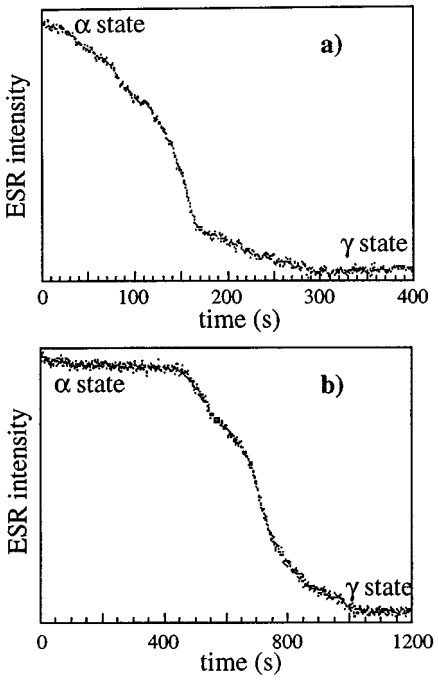

FIG. 7. Fluctuation-induced $\alpha \leftrightarrow \gamma$ transition in β-Ga_2O_3 at 150 K under bistability conditions with $U_\gamma < U_\alpha$. The spin-field system lies in the α state at $t=0$. The variation of the CESR intensity corresponds to the transition to the γ state. (a) $B_0 - h\nu/g\beta = -2.41$ G; (b) $B_0 - h\nu/g\beta = -2.68$ G.

Without precise information on the characteristics of fluctuations, we may assume that $\eta(t)$ corresponds to the most general Gaussian white noise with zero mean value and a δ-autocorrelation function:

$$\langle \eta(t)\rangle = 0,$$

$$\langle \eta(t)\,\eta(t')\rangle = 2D.\delta(t-t'), \tag{13}$$

where D is the variance of fluctuations and $\delta(t-t')$ is the Dirac function. The noise intensity D is independent of time. Equation (12) still corresponds to the overdamped motion of a fictitious particle in the potential U, and submitted to fluctuations.

B. Fokker-Planck equation for the nuclear field

The effect of fluctuations is to induce a distribution of B_n characterized by a distribution probability $W(B_n,t)$, which is solution of a Fokker-Planck equation (FPE):[22]

$$\frac{\partial W(B_n,t)}{\partial t} = \left[-\frac{\partial}{\partial B_n} D^{(1)}(B_n) + \frac{\partial^2}{\partial B_n^2} D^{(2)}(B_n) \right] W(B_n,t), \tag{14}$$

where the terms within brackets represent the Fokker-Planck operator L_{FP}. The terms $D^{(1)}(B_n)$ and $D^{(2)}(B_n)$ are, respectively, the drift coefficient and the diffusion coefficient. In the case of the Overhauser effect with the fluctuation characteristics described above, these coefficients are given by

$$D^{(1)}(B_n) = -\frac{\partial U(B_n)}{\partial B_n},$$

$$D^{(2)}(B_n) = D. \tag{15}$$

The Fokker-Planck equation (14) represents the equation of motion of the fluctuating variable B_n. With the drift and diffusion coefficients given by Eq. (15), it is equivalent to the Smoluchowski equation describing the Brownian motion of a particle in the potential U,[23] which has been largely treated in the literature. By a separation of variables, the distribution function is written $W(B_n,t) = \Phi(B_n)e^{-\nu t}$, which transforms the FPE into the following eigenvalue equation:

$$L_{\mathrm{FP}}\Phi_j(B_n) = -\nu_j\Phi_j(B_n), \tag{16}$$

where $\Phi_j(B_n)$ and ν_j ($j=0,1,2,3,...$) are the eigenfunctions and the eigenvalues of the Fokker-Planck operator L_{FP}. Knowing the two first eigenvalues ν_0 and ν_1, and the first eigenfunction $\Phi_0(B_n)$, we can describe the behavior of the fluctuating, self-organized spin-field system. $\Phi_0(B_n)$ gives the distribution of the nuclear field associated to the eigenvalue $\nu_0=0$:

$$\Phi_0(B_n) = \mathcal{N}\exp\left(-\frac{U(B_n)}{D}\right), \tag{17}$$

where $\mathcal{N}$ is a normalization constant. The other eigenvalues are strictly positive, with ν_1 being of particular interest since it is related to the inverse Kramers time τ_K^{-1}, which represents the transition rate between the two potential wells. If we note $\tau_{\alpha\to\gamma}$ and $\tau_{\gamma\to\alpha}$ the Kramers times for the transitions $\alpha\to\gamma$ and $\gamma\to\alpha$, respectively, ν_1 is given by the sum of the two Kramers rates:

$$\begin{aligned}\nu_1 &= \tau_{\alpha\to\gamma}^{-1} + \tau_{\gamma\to\alpha}^{-1} \\ &= \frac{1}{2\pi}\sqrt{U''_\alpha|U''_\beta|}\exp\frac{-(U_\beta-U_\alpha)}{D} \\ &\quad + \frac{1}{2\pi}\sqrt{U''_\gamma|U''_\beta|}\exp\frac{-(U_\beta-U_\gamma)}{D}.\end{aligned} \tag{18}$$

This expression is valid only if the intensity D of fluctuations is smaller than the potential barrier $U_\beta - U_i$ ($i=\alpha,\gamma$).

Figure 8 shows the variation of the probability density $(\Phi_0(B_n))^2$ of the distribution of B_n for different magnetic field values corresponding to the BCESR spectrum of Fig. 2(b), and calculated by using expression (17) with a noise intensity $D=0.3\ \mathrm{G}^2\,\mathrm{s}^{-1}$. It can be seen that for $B_0 > B_0^{\uparrow}$ (case a) or $B_0 < B_0^{\downarrow}$ (case e) corresponding to monostable situations, B_n has a nearly Gaussian distribution centered on the stationary nuclear fields B_n^{γ} and B_n^{α}, respectively. For the bistability situation $B_0^{\downarrow} < B_0 < B_0^{\uparrow}$ (cases b, c, and d), B_n is distributed over the two potential wells with a relative weight depending on the difference $U_\alpha - U_\gamma$. Thus the BCESR intensity without fluctuations and with fluctuations are very different. In the former case it is given by the second derivative U''_α and U''_γ of the potential wells [expression (11)]. In the presence of fluctuations, the BCESR intensity (which is no longer bistable) is obtained by integrating, over the nuclear field, the intensity affected by the distribution of the nuclear field. The long-time CESR intensity is thus given by

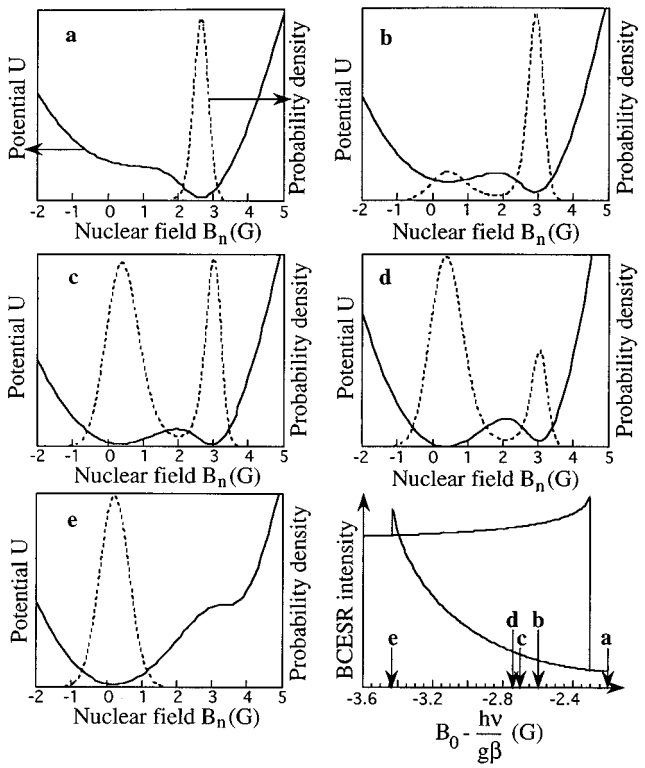

FIG. 8. Variation of the dynamic potential U (full line) and of the probability density $(\Phi_0(B_n))^2$ for the distribution of the nuclear field, vs the nuclear field B_n for β-Ga_2O_3 at 150 K. Each figure is characterized by a value of B_0. These values are marked by arrows in the bottom right figure, which represents the calculated BCESR spectrum. Cases (a) and (e) correspond to monostable situations. Cases (b), (c), and (d) correspond to situations close to the equipotential condition $U_\alpha = U_\gamma$. The parameters of the calculation are the same as for the other figures, with a fluctuation intensity $D=0.3\ \mathrm{G}^2\,\mathrm{s}^{-1}$.

$$\frac{I_{\mathrm{ESR}}(B_0,D)}{I_0} = \frac{\int_{-\infty}^{+\infty}\exp[-U(B_n,B_0)/D]I_{\mathrm{ESR}}(B_n,B_0)dB_n}{I_0\int_{-\infty}^{+\infty}\exp[-U(B_n,B_0)/D]dB_n}. \tag{19}$$

Figure 9 represents the theoretical and experimental CESR intensities for β-Ga_2O_3 at 150 K in the small magnetic field range of the bistability window where fluctuation effects are present. This field range corresponds to $U_\gamma < U_\alpha$. The full line represents the BCESR intensity without fluctuations ($D=0$) given by expression (11). The other curves represent the stationary CESR intensities given by expression (19) for different values of the fluctuation intensity D. The experimental points were measured by following the evolution of the CESR intensity at fixed values of B_0 (Fig. 7). In each case the spin system was prepared in the α state at time $t=0$ by a positive variation of B_0. The CESR intensities at $t=0$ and $t=+\infty$ are represented in Fig. 9 by open circles and full circles, respectively. It appears that $D=0.3\ \mathrm{G}^2\,\mathrm{s}^{-1}$ is a good guess, even though we lack experimental data for the magnetic field range corresponding to the equipotential ($U_\alpha \approx U_\gamma$), due to the very long time required for these ex-

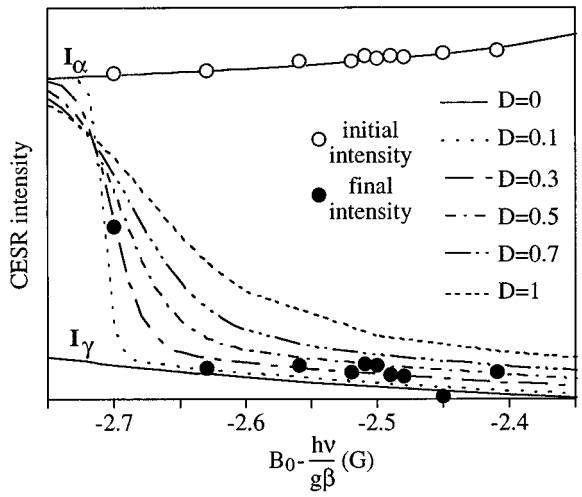

FIG. 9. Calculated and experimental CESR intensity vs B_0 taking into account the effect of fluctuations of the nuclear field, for β-Ga_2O_3 at 150 K under bistability conditions. The magnetic field range corresponds to the bistability window $B_0^{\downarrow}<B_0<B_0^{\uparrow}$. Each curve is calculated with a fixed value of the fluctuation intensity D (in $G^2\,s^{-1}$). The experimental points represented by open circles ($t=0$) and full circles ($t=+\infty$) correspond to the CESR intensity measured on curves such as those shown in Fig. 7. The experimental values at $t=+\infty$ are compatible with a fluctuation intensity $D=0.3\pm0.2\ G^2\,s^{-1}$.

periments. In this case the response is most sensitive to instrumental fluctuations. The fact that the experimental value of D is smaller than the potential barrier justifies the assimilation of the eigenvalue ν_1 of Eq. (16) with the Kramers rate [expression (18)].

It should be noted that Eq. (2) implies that the steady-state field values B_n^{α} and B_n^{γ} are always positive. However, fluctuations allow negative values for B_n, as can be seen in Fig. 8.

VII. SCHRÖDINGER EQUATION OF THE SELF-ORGANIZED SPIN-FIELD SYSTEM

A. Background

The eigenvalue equation (16) is closely similar to a Schrödinger equation, except that the Fokker Planck operator is generally not Hermitian. This property can be achieved by the following transformation.[22]

$$\mathcal{H}=\exp\left(-\frac{U(B_n)}{2D}\right)L_{\mathrm{FP}}\exp\left(\frac{U(B_n)}{2D}\right), \tag{20}$$

where $\mathcal{H}$ is now a Hamiltonian. Applying transformation (20) to the stationary FPE (16) gives the following Schrödinger equation:

$$\mathcal{H}\Psi_j(B_n)=-\nu_j\Psi_j(B_n) \tag{21}$$

with the same eigenvalues as Eq. (16). The eigenfunctions $\Psi_j(B_n)$ of the Hamiltonian $\mathcal{H}$ are related to the eigenfunctions $\Phi_j(B_n)$ of the Fokker-Planck operator L_{FP} by the transformation:

$$\Psi_j(B_n)=\exp\left(\frac{U(B_n)}{D}\right)\Phi_j(B_n). \tag{22}$$

In particular the eigenfunction $\Psi_0(B_n)$ corresponding to the first eigenvalue $\nu_0=0$, which gives the stationary distribution of B_n, is derived from expressions (17) and (22):

$$\Psi_0(B_n)=\mathcal{N}\exp\left(-\frac{U(B_n)}{2D}\right). \tag{23}$$

It is the only eigenfunction of $\mathcal{H}$ which can be determined analytically in the most general case for the Schrödinger equation (21). However, $\mathcal{H}$ being Hermitian, its eigenfunctions form a complete set characterized by the orthonormality relation (24) and the completeness relation (25):

$$\int \Psi_j(B_n)\Psi_k(B_n)dB_n=\delta_{jk}, \tag{24}$$

$$\sum_j \Psi_j(B_n)\Psi_j(B_n)=\delta(B_n-B_n). \tag{25}$$

Applying transformation (20) to the Fokker-Planck operator L_{FP} [expression (14)] leads to the following Hamiltonian for the spin-field system:

$$\mathcal{H}=D\frac{\partial^2}{\partial B_n^2}-V_S(B_n), \tag{26}$$

where $D\partial^2/\partial B_n^2$ represents a ''kinetic'' term, and where the Schrödinger potential V_S takes the following form:

$$V_S(B_n)=\frac{(U'(B_n))^2}{4D}-\frac{U''(B_n)}{2}. \tag{27}$$

The conversion of the FPE to a Schrödinger equation gives an interesting physical image for the self-organization of the spin-field system as will be discussed in Sec. VIII. The Hamiltonian (26) can also be written as follows:

$$\mathcal{H}=-a^+a, \tag{28}$$

where the operators a and a^+ are defined by[22]

$$\begin{aligned} a&=\sqrt{D}\,\exp\frac{-U(B_n)}{2D}\frac{\partial}{\partial B_n}\exp\frac{U(B_n)}{2D},\\ a^+&=-\sqrt{D}\,\exp\frac{U(B_n)}{2D}\frac{\partial}{\partial B_n}\exp\frac{-U(B_n)}{2D}, \end{aligned} \tag{29}$$

and with the following commutation relation:

$$[a,a^+]=U''(B_n). \tag{30}$$

This commutator and expression (11) are linked by the following general expression for the CESR intensity:

$$\frac{I_{\mathrm{ESR}}}{I_0}=1-T_x[a,a^+]. \tag{31}$$

Thus a simple examination of the CESR spectrum allows us to determine the value taken by the commutator (30) for

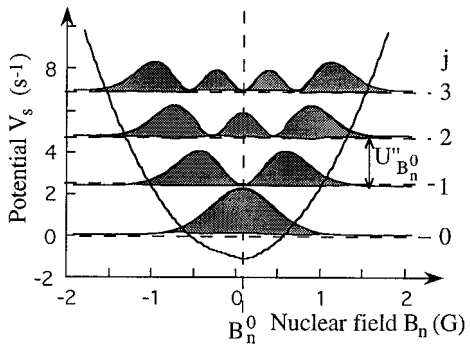

FIG. 10. Harmonic oscillator describing the monostable self-organization of the spin-field system in β-Ga_2O_3 at 300 K, $B_1=0.04$ G, $B_0 \approx h\nu/g\beta$ and $D=0.3$ $G^2\,s^{-1}$. This figure represents the Schrödinger potential V_S, the eigenvalues ν_j ($j=0$–3) and the corresponding probability densities $(\Psi_j(B_n))^2$.

all the different situations of temperature and (static and microwave) magnetic field amplitudes.

B. Monostable self-organization

The interest of describing the self-organization of the spin-field system by a Schrödinger equation can be assessed by considering again the most common situation of monostable Overhauser effect discussed in Sec. V A, which may be described by a harmonic potential U. With transformation (27) the harmonic potential given in expression (10) is converted to a harmonic Schrödinger potential V_S given by

$$V_S = U''_{B_n^0}\left(U''_{B_n^0}\,\frac{(B_n - B_n^0)^2}{4D} - \frac{1}{2}\right). \tag{32}$$

The corresponding commutation relation of operators a and a^+ becomes $[a,a^+]=U''_{B_n^0}$. The analogy with the quantum-mechanical harmonic oscillator can be shown by writing the operators a and a^+ as $a=b\sqrt{U''_{B_n^0}}$ and $a^+ = b^+\sqrt{U''_{B_n^0}}$. The operators b and b^+ obey the well-known commutation relation $[b,b^+]=1$ and are thus strictly equivalent to the creation and annihilation boson operators of quantum mechanics.[24] The Hamiltonian now takes the form

$$\mathcal{H} = -U''_{B_n^0} b^+ b \tag{33}$$

with eigenvalues

$$\nu_j = jU''_{B_n^0} \quad (j=0,1,2,3,\ldots) \tag{34}$$

and eigenfunctions which are those of the harmonic oscillator, given by the usual expressions:

$$\Psi_0(B_n) = \left(\frac{1}{2\pi D T_x}\right)^{1/4} \exp\left(-\frac{B_n^2}{4DT_x}\right),$$
$$\Psi_j(B_n) = \frac{(b^+)^j}{\sqrt{j!}}\,\Psi_0(B_n). \tag{35}$$

Figure 10 shows a monostable Schrödinger potential with the first eigenvalues ν_i and the associated probability densities $(\Psi_j(B_n))^2$. It can be seen that the self-organized states of the spin-field system are quantified, with a quantum equal to $U''_{B_n^0} = \sqrt{2V''_S D}$ and a ground state $\nu_0=0$ lying at half a quantum above the potential origin.

It is worth noticing that the close analogy of the monostable self-organized spin-field system with the quantum-mechanical harmonic oscillator implies the existence of an uncertainty relation. The latter can be obtained from operators b and b^+, which are derived from the a and a^+ operators given by expression (29):

$$b = \frac{1}{\sqrt{2}}\left(\xi + \frac{\partial}{\partial\xi}\right),$$
$$b^+ = \frac{1}{\sqrt{2}}\left(\xi - \frac{\partial}{\partial\xi}\right), \tag{36}$$

with

$$\xi = \sqrt{\frac{U''_{B_n^0}}{2D}}\,(B_n - B_n^0). \tag{37}$$

ξ represents a dimensionless ''position'' operator in the magnetic field space, and its corresponding ''momentum'' operator P is written as $P=-i\partial/\partial\xi$. The calculation of their root-mean-square deviations $\Delta\xi$ and ΔP is straightforward and is found in many text books of quantum mechanics, which gives the following relation:

$$\Delta\xi\Delta P = j + 1/2 \geqslant 1/2. \tag{38}$$

Retaining the analogy of the spin-field self-organization with a quantum-mechanical particle moving in the B_n space, the uncertainty relation (38) originates from the impossibility for the particle to minimize the two terms of the Hamiltonian (26), because the fluctuation intensity D figures in the numerator of the ''kinetic'' term and in the denominator of the potential term [Eq. (27)].

C. Bistable self-organization

In the most general case where no particular conditions are imposed to the microwave field B_1 and to the external field B_0, the Schrödinger potential V_S is no longer harmonic and becomes bistable if the critical condition (4) is satisfied. Figure 11 shows an example of bistable potential V_S calculated from expressions (27) and (9) for different values of D. Its shape is significantly different from that of the dynamic potential. It is worth noticing that the potential wells are more pronounced for V_S than for the dynamic potential U, and that the shape of the former is not strongly dependent on the fluctuation intensity D. In particular this parameter influences only the two limits of V_S. In contrast with the harmonic case, the eigenvalues and eigenfunctions of the general Hamiltonian (26) cannot be derived analytically except for those corresponding to the ground state $j=0$, with $\nu_0=0$ and $\Psi_0(B_n)$ given by expression (23). The ground-state probability distribution $(\Psi_0(B_n))^2$ for the nuclear field calculated with $D=0.3$ $G^2\,s^{-1}$ is shown in Fig. 11. Like the harmonic oscillator, the ground state ν_0 lies above the bottom of

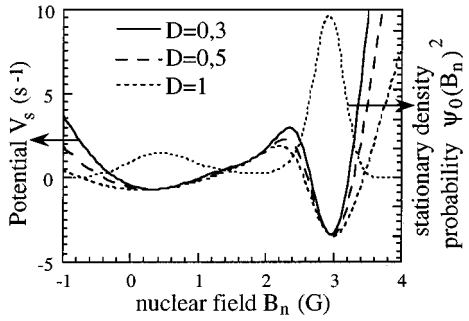

FIG. 11. Anharmonic oscillator describing the bistable self-organization of the spin-field system in β-Ga_2O_3 at 150 K, $B_1=0.4$ G, and $B_0-h\nu/g\beta=-2.6$ G. This figure represents the Schrödinger potential V_S calculated for different values of D (in $G^2\,s^{-1}$), with the ground-state eigenvalue ν_0 and the corresponding probability density $(\Psi_0(B_n))^2$ calculated for $D=0.3\ G^2\,s^{-1}$.

the potential. This feature can also be interpreted by the fact that it is impossible for the self-organized spin-field system to minimize both the ''kinetic term'' and the ''potential term'' of its Hamiltonian.

VIII. MOLECULAR ANALOGY

The same type of Hamiltonian as in Eq. (26) is found in many situations, among which molecular systems are the most familiar to chemists. For example, the vibrational Hamiltonian of a diatomic molecule A-B is written, within the adiabatic approximation,

$$\mathcal{H}=\frac{P^2}{2\mu}+V(Q-Q_e), \tag{39}$$

where $\mu=M_AM_B/(M_A+M_B)$ is the reduced mass of the molecule, Q and Q_e are, respectively, the configuration coordinate (the interatomic distance) and its equilibrium value, and $P=-i\hbar d/dQ$ is the momentum operator. The potential $V(Q-Q_e)$ corresponds to the ground-state electronic energy. It exhibits a characteristic shape (Morse potential) for a diatomic molecule. However, restricting the molecular vibrations to small oscillations about the equilibrium interatomic distance Q_e, the expansion of the potential V about Q_e may be restricted to its harmonic term $V\approx V''_{Q_e}(Q-Q_e)^2/2=\mu\omega^2(Q-Q_e)^2/2$. With this restriction, the molecular Hamiltonian (39) is strictly equivalent to the Hamiltonian (26) of the monostable spin-field system discussed in Sec. VII. The nuclear field B_n and its steady-state value B_n^0 correspond, respectively, to the configuration coordinates Q and Q_e. The term $D\partial^2/\partial B_n^2$ for the spin-field system corresponds to the kinetic energy $P^2/2\mu=(\hbar^2/2\mu)d^2/dQ^2$ of the molecule, giving the expression $\mu=\hbar^2/2D$ for the ''reduced mass'' of the self-organized spin-field system. With this analogy, the vibrational quantum $\hbar\omega$ of the ''spin-field molecule'' is equal to $\hbar\sqrt{2V''_SD}$. The vibrational wave function $\Psi_j(Q)$ of the molecule, which represents the indetermination on the interatomic distance in the jth vibrational level, is equivalent to the distribution probability $\Psi_j(B_n)$ for the nuclear field.

The molecular analogy of the self-organized spin-field system extends to the bistable case (Fig. 11). Bistable electronic ground states are known for a variety of dinuclear transition metal complexes called mixed-valence complexes.[25,26] Let us write A-B as such a complex, with one electron being trapped on one of the two sites A or B. The two stable states of the complex are written $A^\circ-B$ and $A-B^\circ$ depending on the electron site. The corresponding electron energy $V(Q)$ exhibits a double-well contour with minima at configuration coordinates Q_A and Q_B. Depending on the chemical nature of A and B, the potential takes a variety of shapes including those encountered for the bistable spin-field system, where Q_A and Q_B are substituted by the steady-state nuclear fields B_n^α and B_n^γ. The thermally activated electron transfer $A^\circ-B\leftrightarrow A-B^\circ$ between the two sites is equivalent to the fluctuation induced $\alpha\leftrightarrow\gamma$ switching of the spin-field system, the role of kT being played by the fluctuation intensity D. Recently Guihery *et al.*[15] discussed the possibility of using bistable donor-acceptor molecular complexes for bit storage, the switching between the two states being induced by the application of an external perturbation which modifies the shape of the potential. This is strictly equivalent to the modification of the potential U (or V_S) induced by the field sweeping in BCESR, where B_0 plays the role of the external perturbation.

Contrary to molecular systems which exhibit discrete electron energy levels (discrete potentials V), the spin-field system possesses an infinity of potentials since a potential is determined by the values of the external parameters B_0, B_1, and T, which are continuous parameters. However the rapid modification of a control parameter induces a vertical transition from one potential to another [see Fig. 6(a) and examples shown in Ref. 14]. This is equivalent to the vertical transitions between electronic molecular states (Franck-Condon principle) in molecular spectroscopy.

IX. CONCLUSION AND PERSPECTIVES

The purpose of this work is to analyze the Overhauser effect in conductors in terms of self-organization of the system composed of nuclear spins and the microwave field B_1. Saturation of the ESR line of the conduction electron spins induces an ordering of the nuclear spins, resulting in an enhanced nuclear field which shifts and distorts the ESR line. Two situations are analyzed. The first corresponds to the monostable Overhauser effect, which is the most common situation known so far, and in which the resonance line is only shifted and distorted but exhibits no hysteresis. The second situation corresponds to the bistable Overhauser effect, which was easily produced at high temperatures and moderate fields only in gallium oxide. The nuclear field is bistable and its actual value depends on the direction of the magnetic field sweep. The corresponding CESR line is strongly distorted and exhibits hysteresis.

We focused on the behavior of the dynamics of nuclear spins including the effect of fluctuations. The principal results are the following:

(i) By restricting the dynamics to its deterministic aspect, the enhancement of the nuclear field is interpreted as an overdamped motion in a potential U, which is monostable or bistable depending on internal and external parameters.

(ii) The second derivative of the potential is directly related to the CESR intensity by a very simple expression. Under steady-state nuclear polarization, the shape of monostable and bistable CESR spectra are determined by the second derivative at the minima of U. The transient CESR intensity is determined by the second derivative of U along the trajectory of the spin-field system in the potential.

(iii) Fluctuations of the nuclear field induce transitions between the two potential wells, so that they influence the long-time behavior of the BCESR spectrum. The effect of fluctuations is taken into account in the dynamics by solving the Fokker-Planck equation for the spin-field system, which gives the stationary distribution of the nuclear field.

(iv) When the Fokker-Planck equation is converted into a Schrödinger equation, the self-organized spin-field system may be compared to a vibrating molecular system in the nuclear field space. The nuclear field plays the role of the configuration coordinate. With this description, the monostable and bistable spin-field systems correspond to diatomic and mixed-valence molecular architectures respectively.

In conclusion, the bistable Overhauser effect offers a very simple situation where the combination of deterministic and stochastic effects could be studied with routine experimental setup. In particular the phenomenon of stochastic resonance has attracted a considerable attention over the last decade.[27] Basically, this effect is the response of a bistable system to a weak periodic modulation and to an external noise. Contrary to linear systems, the signal-to-noise ratio of the response of the bistable system increases with the noise intensity up to a maximum, and next decreases for further increase of the noise intensity. The bistable Overhauser effect could provide the possibility of observing the stochastic resonance in an electron spin-nuclear spin system.

ACKNOWLEDGMENTS

Laboratorie de Chimie Appliquée de l'Etat Solide is Unité Associée au Centre National de la Recherche Scientifique No. 1466.

*Author to whom correspondence should be addressed.

[1] G. Feher and A. F. Kip, Phys. Rev. **98**, 337 (1955).
[2] A. Overhauser, Phys. Rev. **96**, 411 (1953).
[3] I. Solomon, Phys. Rev. **99**, 559 (1959).
[4] C. Ryter, Phys. Rev. **5**, 10 (1960).
[5] B. Clergeaud, F. Gendron, H. Obloh, J. Schneider, and W. Wilkening, Phys. Rev. B **40**, 404 (1989); G. Denninger and H. Pascher, Solid State Commun. **70**, 399 (1989).
[6] B. Gotschy and G. Denninger, Mol. Cryst. Liq. Cryst. **237**, 435 (1993).
[7] J. I. Kaplan, Phys. Rev. **99**, 1322 (1955).
[8] M. Gueron and C. Ryter, Phys. Rev. Lett. **3**, 338 (1959).
[9] E. Aubay and D. Gourier, J. Phys. Chem. **96**, 5513 (1992).
[10] E. Aubay and D. Gourier, Phys. Rev. B **47**, 15 023 (1993).
[11] L. Binet, D. Gourier, and C. Minot, J. Solid State Chem. **111**, 420 (1994).
[12] E. Aubay and D. Gourier, Solid State Commun. **85**, 821 (1993).
[13] H. Haken, *Synergetics* (Springer-Verlag, Berlin, 1983).
[14] D. Gourier, E. Aubay, and J. Guglielmi, Phys. Rev. B **50**, 2941 (1994).
[15] N. Guihery, G. Durand, M. B. Lepetit, and J. P. Malrieu, Chem. Phys. **183**, 61 (1994).
[16] A. Portis, Phys. Rev. **91**, 1071 (1953).
[17] This expression is oversimplified. It must take into account the existence of several isotopes and the composition of the conduction band. A more precise expression is given in Refs. 10 and 11.
[18] L. Binet, D. Massiot, and D. Gourier (unpublished).
[19] H. A. Kramers, Physica **7**, 284 (1940).
[20] A. Abragam, *Principles of Nuclear Magnetism* (Clarendon, Oxford, 1983), p. 369.
[21] L. Landau and E. Lifchitz, *Mécanique* (Mir, Moscou, 1966).
[22] H. Risken, *The Fokker-Planck Equation* (Springer, Berlin, 1984).
[23] M. Von Smoluchowski, Ann. Phys. (Leipzig) **21**, 756 (1906).
[24] A. Messiah, *Quantum Mechanics* (North-Holland, Amsterdam, 1991).
[25] N. S. Hush, Prog. Inorg. Chem. **8**, 357 (1967).
[26] S. B. Piepho, E. R. Krausz, and P. N. Schatz, J. Am. Chem. Soc. **100**, 2996 (1978).
[27] See, for example, M. I. Dykman, D. G. Luchinsky, R. Manella, P. V. E. McClintock, N. D. Stein, and N. G. Stocks, Nuovo Cimento **17**, 661 (1995), and references therein.